Optimization design and experiment on feeding and chopping device of silage maize harvester

Meizhou Chen[1], Guangfei Xu[2], Maojian Wei[1], Xiaowei Li[2], Yuanzhen Wei[3], Peisong Diao[1*], Peide Cui[1], Shaomin Teng[4]

(1. *College of Agricultural Engineering and Food Science, Shandong University of Technology, Zibo 255000, Shandong, China*;
2. *School of Mechanical and Automotive Engineering, Liaocheng University, Liaocheng 252000, Shandong, China*;
3. *Shandong Academy of Agricultural Machinery Sciences, Jinan 250000, China*;
4. *Menoble Co., Ltd., Beijing 100010, China*)

Abstract: Horizontal feeding devices and plate hob chopping devices are the key component of silage maize harvester. To solve the problem of feeding blockage, reduce energy consumption, and improve the chopping quality of the chopping device a horizontal different diameter five-rollers device (HDDFD) was designed and the plate hob chopping device was simultaneously optimized and analyzed. Through the dynamic analysis, the feeding conveying speed was determined to be 2.0-4.5 m/s. The distance equation of the actual and theoretical cutting-edge curve and the position of the fixed blade were finally obtained. Single factor and response surface orthogonal tests in the bench site were carried out with feeding speed, rotating speed of chopping cylinder, feeding amount, and feeding direction as influencing factors, standard grass length rate (SGLR), and energy consumption per unit mass (ECPUM) as evaluation indexes. The optimal working parameters for chopping performance could be concluded as a feeding speed of 3.39 m/s, rotating speed of the chopping cylinder of 1016.17 r/min, feeding amount of 8.04 kg/s, and feeding direction of 52.2°. In addition, the SGLR and ECPUM were obtained as 95.35% and 37.63 kJ/kg, respectively. The relative error between the experimental results with round parameter combination and the predicted value was verified to be less than 5%. Field tests verified the reliability of the optimized feeding and chopping device. It can be seen that the HDDFD and optimized plate hob chopping device can meet the requirements of mechanized silage harvesting which obviously improves the working quality and reduce the energy consumption of chopping.

Keywords: silage maize, feeding device, chopping device, stand grass length ratio, energy consumption
DOI: 10.25165/j.ijabe.20231603.7922

Citation: Chen M Z, Xu G F, Wei M J, Li X W, Wei Y Z, Diao P S, et al. Optimization design and experiment on feeding and chopping device of silage maize harvester. Int J Agric & Biol Eng, 2023; 16(3): 64–77.

1 Introduction

Silage maize is known as the "king of feed" because it is rich in crude protein, sugar, carotene, and other nutrients. It is an indispensable feed source for the production of dairy and meat worldwide[1,2]. The quality of field mechanized harvesting directly affects feed palatable and commodity value[3]. However, there are some problems in China's self-contained silage maize harvester, such as feeding blockage, high energy consumption, and poor quality of chopping, which seriously affect the quality and efficiency of harvesting[4]. Therefore, it is urgent to optimize and develop the horizontal feeding device and plate hob chopping device.

In the aspect of improving feeding technology, taking the horizontal four-rollers feeding device as the research object, the researches mainly focus on the selection of roller diameter, roller tooth, and optimal design of roller speed[5-9], the matching of the speed characteristics of the front, middle and rear feeding rolls[10-13]. However, the research on structural innovation of feeding devices to solve the problem of blockage has not been found.

In the aspect of improving chopping technology, the researches tend to be aimed at the sliding cutting angle theories[14,15], cutting mechanism[16], cutter shaft structure[17], and other research methods of the rotary cutting device[18]. The effects of working parameters such as harvester forward speed and cutting device speed on cutting performance and power consumption are also studied[19]. There are few researches on the structure optimization of the plate hob chopping device.

In this case, a horizontal different diameter five-rollers feeding device (HDDFD) was designed to increase the feeding interval with the diameter of the up roller larger than the low roller, as well as the moving and fixed blade of the plate hob chopping device was rearranged to make the actual cutting-edge curve closer to the theoretical cutting-edge curve which can help to reduce the cutting energy consumption and improve the cutting quality. The reliability of the optimized feeding and chopping device was verified by bench test and field test, and the best working parameters were obtained.

Received date: 2022-09-17 **Accepted date:** 2023-04-24
Biographies: Meizhou Chen, PhD, Lecturer, research interest: agricultural machinery and equipment, Email: chenfeng2830@163.com; **Guangfei Xu**, PhD, research interest: intelligent agricultural manufacturing, Email: gfxu@sdut.edu.cn; **Maojian Wei**, MS candidate, research interest: agricultural machinery, Email: wmjsyjs2020@163.com; **Xiaowei Li**, MS candidate, research interest: agricultural machinery, Email: 921878985@qq.com; **Yuanzhen Wei**, MS, research interest: agricultural machinery, Email: 549460141@qq.com; **Peide Cui**, MS candidate, research interest: agricultural machinery, Email: 1220830601@qq.com; **Shaomin Teng**, MS, research interest: agricultural machinery, Email: 415237290@qq.com.

***Corresponding author: Peisong Diao**, PhD, Professor, research interest: agricultural mechanization engineering. College of Agricultural Engineering and Food Science, Shandong University of Technology, Zibo 255000, Shandong, China. Tel: +86-13864306142, Email: dps2003@163.com.

2 Mechanism analysis of HDDFD

2.1 Structure of HDDFD

The scheme of horizontal five-roller feeding device of different diameters is shown in Figure 1, including the up-grabbing roller, up feeding roller, low feeding roller, intermediate conveyor roller, and low grabbing roller (five-rollers). Among them, in order to improve the ability of grabbing crops without increasing the gravity center of feeding device, the diameter of up grabbing roller is larger than that of low grabbing roller and inclined arrangement vertically.

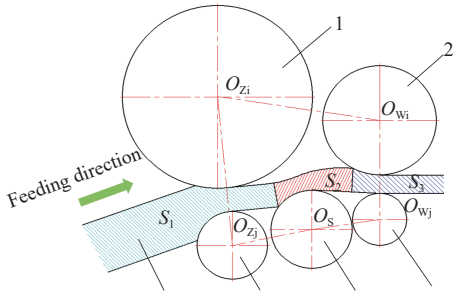

Note: O_{Zi}, O_{Zj}, O_S, O_{Wi}, O_{Wj} are centers of up grabbing roller, low grabbing roller, intermediate conveyor roller, up feeding roller, low feeding roller, separately; S_1, S_2, and S_3 are the grabbing, intermediate conveying, feeding region of feeding device, separately.

1.Up grabbing roller 2.Up feeding roller 3.Low feeding roller 4.Intermediate conveyor roller 5.Low grabbing roller 6.Silage maize

Figure 1 Schematic diagram of horizontal five-rollers feeding device of different diameters

In order to adapt to the fluctuation of feeding amount and increase the residence time of crops in the feeding device, an intermediate conveying roller is added to balance the space generated by the difference between up and low rollers. According to the different functions of each roller, the feeding device is divided into grabbing, intermediate conveyor, and feeding region. In particular, the up grabbing roller and up feeding roller were floating spring designs.

The structure of the feeding device is shown in Figure 2. According to the different functions of each part, the up grabbing roller was triangular blade, the low grabbing roller was trapezoidal tooth, the intermediate conveyer roller and up feeding roller were groove tooth roller, and the low feeding roller was light roller.

2.2 Dynamic analysis of grabbing process

In the grabbing region, the function of up and low-grabbing rollers is to grab the silage maize continuously sent by the header to the feeding device with preliminary flattening and crushing, so as to improve the grabbing ability of disorderly crops and avoid the blockage phenomenon due to feeding failure. Crops have no thrust and only rely on the force of grabbing rollers in the process of grabbing[12]. Therefore, mechanical analysis is needed to determine the parameters of each mechanism meeting the grabbing conditions. The coordinate system is established and the force analysis was carried out on silage maize in the grabbing region, as shown in Figure 3. Therefore, the mathematical calculation model of the force acting on silage maize along the x-direction F_{Zx} was as follows:

$$F_{Zx}=\int_0^{t_1}(F_{Zix}-f_{Zi})\mathrm{d}T+\int_0^{t_1'}\left(F_{Zjx}-f_{Zj}\right)\mathrm{d}T \tag{1}$$

The up grabbing roller was set as a floating roller to avoid clogging due to silage maize feeding too much. At this point, the forces of up grabbing roller and silage maize are balanced in the y-direction, and the equilibrium equations in y-direction are

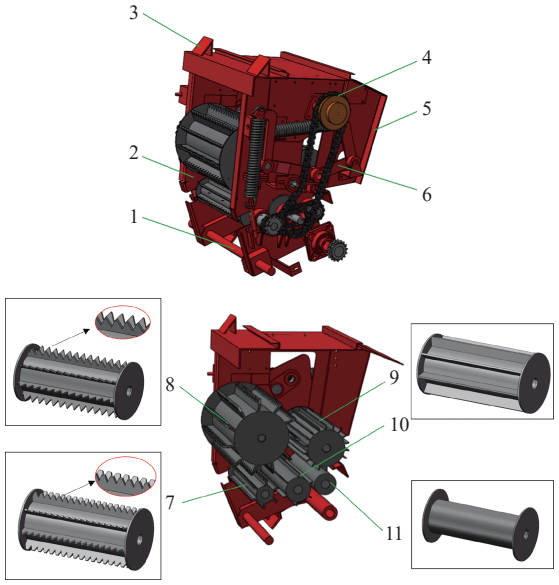

1. Hitch mechanism 2. Rack 3. Upper suspension mechanism 4. Transmission system 5. Feeding inlet 6. Copying institutions 7. Low grabbing roller 8. Up grabbing roller 9. Up feeding roller 10. Intermediate conveyor 11. Low feeding roller

Figure 2 Structure of horizontal five-roller feeding device of different diameters

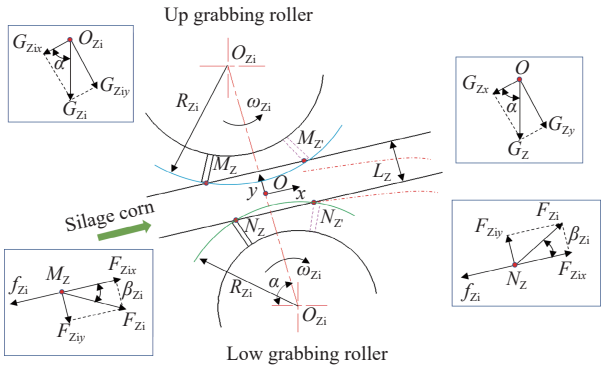

Note: R_{Zi}, R_{Zj} are the radius of up and low grabbing rollers, mm; ω_{Zi}, ω_{Zj} are the angular velocity of up and low grabbing rollers, rad/s; α is the angle between the line of up and low grabbing rollers, (°); M_Z, N_Z are the initial contact point between five-rollers and silage maize; M_Z', N_Z' are the separation point between rollers and silage maize; G_{Zi} is the gravitational force of up grabbing roller, N; G_{Zix} G_{Ziy} are the component gravitational force of up grabbing roller along x- and y-axis, N; G_{Wix}, G_{Wi} are the component gravitational force of up feeding roller along the x-, y-axis, N; G_Z is the gravitational force of silage maize in grabbing region, N; G_{Zx}, G_{Zy} are the component gravitational force of G_Z along x-axis and y-axis, N; F_{Zi}, F_{Zj} are the force of up and low grabbing rollers on silage maize, N; F_{Zix}, F_{Zjx} are the component force of F_{Zi}, F_{Zj} along the x-axis, N; F_{Ziy}, F_{Zjy} are the component force of F_{Zi}, F_{Zj} along the y-axis, N; f_{Zi}, f_{Zj} are the frictional force of five-rollers on silage maize, N; β_{Zi}, β_{Zj} are the angle between the tangent direction of up and low grabbing rollers on silage maize along the x-axis, (°); L_Z is thickness of silage maize layer leaving grabbing region, intermediate conveyor region, feeding region, mm.

Figure 3 Force analysis diagram of silage maize between up and low grabbing rollers

$$\begin{cases}F_{Ziy}=G_{Zi}\sin\alpha\\ F_{Zjy}=F_{Ziy}+G_{Zy}\end{cases} \tag{2}$$

$$\begin{cases} G_{Zi} = m_{Zi}g \\ G_{Zy} = m_Z g\sin\alpha \end{cases} \tag{3}$$

Substituting Equation (2) into Equation (3), the following equations can be obtained.

$$\begin{cases} F_{Ziy} = m_{Zi}g\sin\alpha \\ F_{Ziy} = (m_{Zi}+m_Z)g\sin\alpha \end{cases} \tag{4}$$

$$\begin{cases} F_{Zix} = F_{Ziy}\cot\beta_{Zi} \\ F_{Zjx} = F_{Zjx}\cot\beta_{Zj} \\ f_{Zi} = \lambda_{Zi}F_{Ziy} \\ f_{Zj} = \lambda_{Zj}F_{Zjy} \\ G_{Zx} = m_Z g\cos\alpha \end{cases} \tag{5}$$

Substituting Equation (5) into Equation (4), the following equation can be obtained.

$$\begin{aligned} F_{Wx} = &\int_0^{t_3}(F_{Wix}-f_{Wi})d\mathrm{T} + \int_0^{t'_3}\left(F_{Wjx}-f_{Wj}\right)d\mathrm{T} - G_{Wx} = \\ &\int_0^{t_3}\left(m_{Wi}g\sin\alpha''\cot\delta_{Wi} - \lambda_W m_{Wi}g\sin\alpha''\right)d\mathrm{T} + \\ &\int_0^{t'_3}\left[(m_{Wi}+m_W)g\sin\alpha''\cot\delta_{Wj} - \lambda_W(m_{Wi}+m_W)g\sin\alpha''\right]d\mathrm{T} - \\ &m_W g\cos\alpha'' = m_{Wi}g\sin\alpha''\int_0^{t_3}(\cot\delta_{Wi}-\lambda_W)d\mathrm{T} + (m_{Wi}+ \\ &m_W)g\sin\alpha''\int_0^{t'_3}(\cot\delta_{Wi}-\lambda_W)d\mathrm{T} - m_W g\cos\alpha'' \end{aligned} \tag{6}$$

From Equation (6), it can be seen that the force acting on silage maize along the x-direction is related to the mass of up grabbing roller m_{Zi} and silage maize in grabbing region m_Z, the angle between the line of up and low grabbing rollers α, angle between the tangent direction of up and low grabbing rollers on silage maize along x-axis β_{Zi} and β_{Zj}, their coefficient of friction λ_{Zi} and λ_{Zj}.

2.3 Dynamic analysis of grabbing process

In the intermediate conveying region, the function of the intermediate conveyor roller is to lengthen the feeding space so that the silage maize can stay long enough to prevent blockage and balance the space generated by the difference between large up grabbing roller and small low grabbing roller. Therefore, the mechanical analysis was carried out on silage maize to determine the parameters of the intermediate conveyor roller in the intermediate conveying region, as shown in Figure 4. Therefore, the mathematical calculation model of the force acting on silage maize along x-direction F_{Ix} was as follows:

$$F_{Ix} = \int_0^{t_2}(F_{Sx}-f_S)\mathrm{d}T - G_{Sx} \tag{7}$$

The force of intermediate conveyor roller and silage maize was balanced in y-direction, the equilibrium equations are:

$$F_{Sy} = G_{Sy} = G_S\sin\alpha' = m_S g\sin\alpha' \tag{8}$$

$$\begin{cases} F_{Sx} = F_{Sy}\cot\gamma_S \\ f_S = \lambda_S F_{Sy} \end{cases} \tag{9}$$

$$F_{Ix} = \int_0^{t_2}(m_S g\sin\alpha'\cot\gamma_S - \lambda_S m_S g\sin\alpha')\mathrm{d}T - m_S g\cos\alpha' \tag{10}$$

When t_2=0, that is after the silage maize is sent to the intermediate conveyor area, Equation (10) becomes

$$F_{Ix} = F_S\cos\gamma_S - f_S - G_S\cos\alpha' \tag{11}$$

Equation (11) shows that with the rotation of the intermediate conveyor roller, γ_S gradually decreases, so the acting force in the conveying direction of silage maize gradually increases.

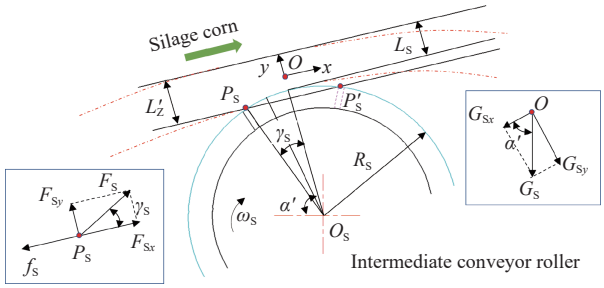

Note: R_S is radius of intermediate conveyor roller, mm; ω_S is angular velocity, rad/s; α' is angle between the line of intermediate conveyor roller with horizontal direction, (°); P_S, P'_S are initial and separation contact point between intermediate conveyor roller and silage maize; G_S is gravitational force of silage maize in intermediate conveyor region, N; G_{Sx}, G_{Sy} are component gravitational forces of G_Z, G_S along x-axis and y-axis, N; F_S is force on silage maize, N; F_{Sx}, F_{Sy} are component forces of F_S along x-axis and y-axis, N; f_S is frictional force of intermediate conveyor roller on silage maize, N; L'_Z is the thickness of silage maize layer leaving grabbing region, mm; L_S is the thickness of silage maize layer entering feeding region, mm; γ_S is the angle between tangent direction of intermediate conveyor roller on silage maize, (°).

Figure 4 Force analysis diagram of silage maize on the intermediate conveyor roller

2.4 Dynamic analysis of feeding process

In the feeding region, the function of up and low feeding rollers is to compress the silage maize further and feed them into the chopping device smoothly and reliably to ensure the quality of chopping. Therefore, the mechanical analysis is shown in Figure 5. Therefore, the mathematical calculation model of the force acting on silage maize along x-direction F_{Wx} was as follows:

$$F_{Wx} = \int_0^{t_3}(F_{Wix}-f_{Wi})\mathrm{d}T + \int_0^{t'_3}\left(F_{Wjx}-f_{Wj}\right)\mathrm{d}T - G_{Wx} \tag{12}$$

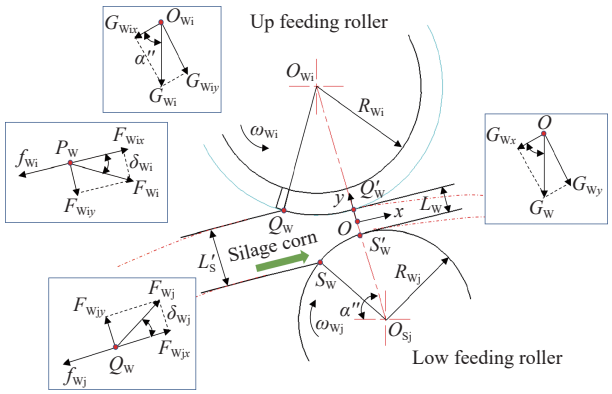

Note: R_{Wi}, R_{Wj} are radius of up and low feeding rollers, mm; ω_{Wi}, ω_{Wj} are angular velocities, rad/s; α'' is angle between line of up and low feeding rollers with horizontal direction, (°); Q_W, S_W are initial contact points; Q'_W, S'_W are separation points; G_{Wi} is gravitational force of up feeding roller, N; G_{Wix}, G_{Wi} are component gravitational forces of up feeding roller along x-, y-axis, N; G_W is gravitational force of silage maize in grabbing region, intermediate conveyor region, N; G_{Wx}, G_{Wy} are component gravitational forces of G_W along x, y-axis, N; F_{Wi}, F_{Wj} are forces of up feeding roller on silage maize, N; F_{Wix}, F_{Wjx} are component forces of F_{Wi}, F_{Wj} along x-axis, N; F_{Wiy}, F_{Wjy} are component forces of F_{Wi}, F_{Wj} along y-axis, N; f_{Wi}, f_{Wj} are frictional forces of five-rollers on silage maize, N; L'_S is thickness of silage maize layer entering the feeding region, mm; L_W is the thickness of silage maize layer leaving feeding region, mm.

Figure 5 Force analysis diagram of silage maize between up and low feeding rollers

Because the up feeding roller fluctuates during the feeding process, the forces on the up feeding roller and silage maize were balanced in *y*-direction. Therefore, it can be obtained that:

$$\begin{cases} F_{\mathrm{Wiy}} = G_{\mathrm{Wi}} \sin\alpha'' \\ F_{\mathrm{Wjy}} = F_{\mathrm{Wiy}} + G_{\mathrm{Wy}} \end{cases} \tag{13}$$

$$\begin{cases} G_{\mathrm{Wi}} = m_{\mathrm{Wi}} g \\ G_{\mathrm{Wiy}} = m_{\mathrm{W}} g \sin\alpha' \end{cases} \tag{14}$$

Substituting Equation (14) into Equation (13) to get Equation (15).

$$\begin{cases} F_{\mathrm{Wiy}} = m_{\mathrm{Wi}} g \sin\alpha'' \\ F_{\mathrm{Wjy}} = m_{\mathrm{Wi}} g \sin\alpha'' + m_{\mathrm{W}} g \sin\alpha'' = (m_{\mathrm{Wi}} + m_{\mathrm{W}}) \sin\alpha'' \end{cases} \tag{15}$$

From Figure 4, it can be seen that the force of the up and low feeding roller on silage maize in *x*-direction can be expressed as follows:

$$\begin{cases} F_{\mathrm{Wi}x} = F_{\mathrm{Wiy}} \cot\delta_{\mathrm{Wi}} = m_{\mathrm{Wi}} g \sin\alpha'' \cot\delta_{\mathrm{Wi}} \\ F_{\mathrm{Wj}x} = F_{\mathrm{Wjy}} \cot\delta_{\mathrm{Wj}} = (m_{\mathrm{Wi}} + m_{\mathrm{W}}) g \sin\alpha'' \cot\delta_{\mathrm{Wj}} \end{cases} \tag{16}$$

$$\begin{cases} f_{\mathrm{Wi}} = \lambda_{\mathrm{W}} F_{\mathrm{Wiy}} = \lambda_{\mathrm{W}} m_{\mathrm{Wi}} g \sin\alpha'' \\ f_{\mathrm{Wj}} = \lambda_{\mathrm{W}} F_{\mathrm{Wjy}} = \lambda_{\mathrm{W}} (m_{\mathrm{Wi}} + m_{\mathrm{W}}) g \sin\alpha'' \\ G_{\mathrm{W}x} = m_{\mathrm{W}} g \cos\alpha'' \end{cases} \tag{17}$$

It is obtained by Equations (15)-(17):

$$\begin{aligned} F_{\mathrm{W}x} = & \int_0^{t_3} (F_{\mathrm{Wi}x} - f_{\mathrm{Wi}}) d\mathrm{T} + \int_0^{t'_3} (F_{\mathrm{Wj}x} - f_{\mathrm{Wj}}) d\mathrm{T} - G_{\mathrm{W}x} = \\ & \int_0^{t_3} (m_{\mathrm{wi}} g \sin\alpha'' \cot\delta_{\mathrm{wi}} - \lambda_{\mathrm{W}} m_{\mathrm{Wi}} g \sin\alpha'') d\mathrm{T} + \\ & \int_0^{t_3} [(m_{\mathrm{Wi}} + m_{\mathrm{W}}) g \sin\alpha'' \cot\delta_{\mathrm{w}j} - \lambda_{\mathrm{W}} (m_{\mathrm{Wi}} + m_{\mathrm{W}}) g \sin\alpha'')] d\mathrm{T} - \\ & m_{\mathrm{W}} g \cos\alpha'' = m_{\mathrm{wi}} g \sin\alpha'' \int_0^{t_3} (\cot\delta_{wi} - \lambda_{\mathrm{W}}) d\mathrm{T} + (m_{\mathrm{Wi}} + \\ & m_{\mathrm{W}}) g \sin\alpha'' \int_0^{t'_3} (\cot\delta_{wi} - \lambda_{\mathrm{W}} d\mathrm{T} - m_{\mathrm{W}}) g \cos\alpha'' \end{aligned} \tag{18}$$

where, λ_{Zi}, λ_{Zj}, λ_S, λ_{Wi}, λ_{Wj} are the friction coefficient of five-rollers, separately.

It is obtained by Equations (6), (10) and (18) that the resultant force of silage maize in the *x*-direction is:

$$F_x = F_{Zx} + F_{\mathrm{I}x} + F_{Wx} \tag{19}$$

where, F_x is the resultant force of silage on in *x*-direction, N.

According to theorem of momentum,

$$F_x t = m_W v_t - m_W v_0 \tag{20}$$

$$v_t = \frac{F_x t}{m_W} - v_0 \tag{21}$$

Substituting Equation (19) into Equation (21) to obtain Equation (22), the speed of silage maize in conveying direction of the feeding device can be expressed as,

$$v_t = (F_{Zx} + F_{\mathrm{I}x} + F_{Wx}) \frac{t}{m_W} - v_0 \tag{22}$$

According to Equation (22), under the horizontal different diameter five-roller feeding scheme, the theoretical feeding speed range of the low feeding roller was 2.0-4.5 m/s. The optimal feeding speed range still needs to be determined by bench test. It can be seen that the feeding speed is very important to grab, transport, and transport of silage maize to the chopping device.

3 Optimization of plate hob chopping device

3.1 Analysis of moving blade trajectory

The chopping device is the key link of silage maize harvesting and determines the operation performance and power consumption of the whole machine. In view of the current problems of high energy consumption of silage harvesting and uneven straw cutting, it was necessary to analyze the moving blade track and fixed blade position configuration. In order to realize automatic grinding of the moving blade and facilitate the adjustment of the moving and fixed blade gap, the moving blade was flat type, and the fixed blade was straight.

The rotary surface of the moving blade should be cylindrical. Only in this case, the gap between the moving blade and the fixed blade could be the same at each cutting point. The mechanical test of Gorochin shows that sliding cutting saves more effort than tangent effort. In the condition of ensuring the quality of cutting to reduce chopping power consumption, moving blade installation needs to have a certain angel and a larger slip-cutting angle is more likely to push crops to the side[20]. The theoretical track of the moving blade should be a segment on the elliptic curve. When the moving blade is titled, the rotary axis of the moving blade and the axis of the rotation cylinder should not be on the same plane.

The theoretical track of the rotary cylinder and flat plate moving blade was designed as shown in Figure 6a. In xz_0 plane, the theoretical blade edge should be an elliptic curve, and its equation was as follows:

$$\frac{x_0^2}{a^2} + \frac{z_0^2}{c^2} = 1, \ (-R \le x_0 \le R) \tag{23}$$

where, *a* is the half of the short axis, mm, *R*; *c* is the half of the long axis, $R/\sin\theta$, mm; *R* is the radius of the moving knife turning cylinder, mm;

For silage maize with more than 60% moisture content, if the moving blade had the ability to chop and throw chopped crops everywhere, the throwing angle should be satisfied[21]:

$$57^\circ \le \varphi_1 \le \varphi_2 \le 60^\circ \tag{24}$$

Thus, the actual length of the moving blade is as follows:

$$L_{A'B'} = R \sqrt{2 - 2(\cos\varphi_2 \cos\varphi_1 + \sin\varphi_2 \sin\varphi_1) + \left(\frac{(\sin\varphi_2 - \sin\varphi_1)^2}{\tan\alpha} \right)} \tag{25}$$

Assuming that the distance between point *C* (x_c, z_c) on the theoretical curve and the actual cutting-edge curve of the moving blade was the maximum, the slope at point *C* was as follows:

$$z'_{0(z=z_c)} = \frac{-2x_c}{R\sin\alpha \sqrt{1 - \frac{x_c^2}{R^2}}} \tag{26}$$

Also, the line of the actual moving edge should be tangent to the theoretical edge curve, and pass through point *A* of the moving edge, then the equation of the actual cutting-edge line can be expressed as follows:

$$z_0 - R\frac{\sin\varphi}{\sin\alpha} = \frac{-2x_c}{R\sin\alpha \sqrt{\left(1 - \frac{x_c^2}{R^2}\right)}} (x_0 - R\cos\varphi_1) \tag{27}$$

The maximum distance between the actual and the theoretical cutting-edge curve is:

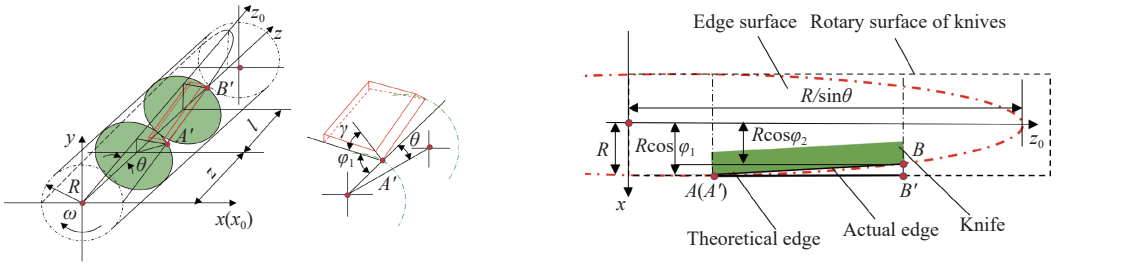

a. Moving knife trajectory

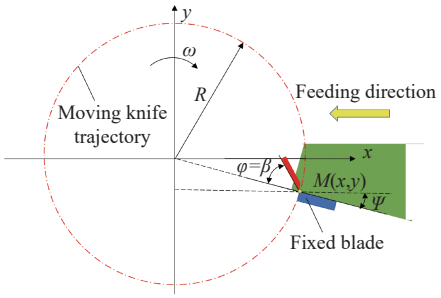

b. Fixed blade position configuration

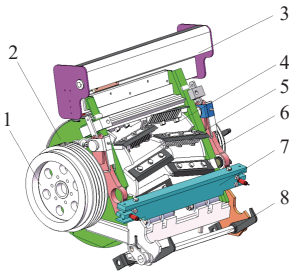

1. Pulley drive 2. Rack 3. Self-grinding device 4. Chopping cylinder
5. Moving blade 6. Clearance adjustment 7. Fixed blade 8. Articulated device

c. Structural diagram of chopping device

Note: $A(A')$ and $B(B')$ are the point on the edge of the moving blade; R is the radius of chopping cylinder, mm; ω is the angular velocity of the chopping cylinder, rad/s; θ is the angle inclination of the moving blade, (°); γ is the edge angle of moving blade, (°); $\varphi_1(\varphi_2)$ is the installation angle of moving blade, (°); z is the coordinates of point A along the long-axis, mm; l is the length of moving blade, mm; β is the angle of chopping angle of moving blade, (°); ψ *is the* angle between fixed blade plane and horizontal plane, (°).

Figure 6 Analysis and determination of moving and fixed blade position

$$d=\frac{\left|-\frac{2x_c^2}{R\sin\theta\sqrt{1-\frac{x_c^2}{R^2}}}-z_0+\frac{2x_c\cos\varphi}{\sin\theta\sqrt{1-\frac{x_c^2}{R^2}}}+\frac{R\sin\varphi}{\sin\theta}\right|}{\sqrt{\frac{2x_c^2}{R^2\sin^2\theta}+1}}=\frac{\left|-\frac{2x_c^2}{\sqrt{R^2-x_c^2}}-z_0\sin\theta\right|}{\sqrt{\frac{2x_c^2}{R^2}+\sin^2\theta}} \tag{28}$$

According to the analysis of the actual moving blade trajectory above, a mathematical model of the distance from the actual cutting-edge straight line to the theoretical cutting-edge curve was established. Combined with the study of the mechanical properties of the whole silage maize, the installation of the plate hob chopping device can be rearranged to reduce the cutting energy consumption and improve the cutting quality.

3.2 Analysis of fixed blade position configuration

The position of moving blade and fixed blade plays an essential role in the chopping quality and energy consumption, and a feeding and chopping prototype system was designed as shown in Figure 6b. The chopping device moves anticlockwise during the chopping process. Actually, when the fixed blade plane and the rotary axis of the moving blade are on the horizontal plane, it is the optimal chopping state point. Through the force analysis, it can be seen that the moving blade tends to push crops outward up from this point, while it tends to drag crops inward down from this point. Therefore, the fixed knife should be configured in the second quadrant, and the thickness of the crop layer should not exceed the plane where the axis of the chopping device is located, so as to ensure that the moving blade does not hinder the feeding of the crop layer in the chopping process, otherwise, the pushing force will increase the chopping power consumption.

When ψ=0, that is, fixed blade is inclined configuration, at this point, φ=β.

$$\begin{cases}\dfrac{x}{R}=\cos\psi\\ \dfrac{|y|}{R}=\sin\psi\end{cases}\Rightarrow\begin{cases}x=R\cos\psi\\ y=-R\sin\psi\end{cases} \tag{29}$$

From Equation (29), the optimal position configuration parameters of the fixed blade were $\{M_2(R\cos\psi, -R\sin\psi), \psi\neq0, \varphi=\beta.\}$.Through the analysis of the position relation and structure of the moving and fixed blades, the chopping device with a moving blade zigzag inclined arrangement was designed, as shown in Figure 6c.

4 Materials and methods

4.1 Test materials and equipment

The test silage maize was “Zhengdan 958”. To simulate the mechanical harvesting process, the silage maize plants were cut from the roots manually, leaving the ears and bracts intact. Some characteristics of its plant are listed in Table 1. The test collection site is shown in Figure 7. When the bench test was carried out, the average moisture content of maize straw, grain, and cob was respectively 65.8%, 38.9%, and 68.2%.

Table 1 Silage maize Parameters

Parameter	Minimum value	Maximum value	Average value
Plant height/mm	2000	2472	2236
Maize ear height/mm	800	1024	912
Ear length/mm	164	220	192
Ear large diameter/mm	44	64	54
Root culm diameter/mm	26	40	33
Plant quality/kg	0.65	0.95	0.8
Maize ear quality/kg	0.28	0.42	0.35

Figure 7 Test material collection site

4.2 Test equipment

In order to verify the feeding and chopping performance of the optimized feeding and chopping device, a test bench was built, as shown in Figure 8.

1. Conveying device 2. Feeding device 3. Chopping device 4. Spilling device 5. Aggregate box 6. Torque and speed acquisition system 7. Chopping motor 8. Feeding motor

Figure 8 Bench test site

The experiment was carried out at Shandong Guofeng, Machinery Co., Ltd, Jining City, Shandong Province, China in June 2021. Test equipment included the bench site, moisture meter (MA100, China), tape measure, electronic scale (JM-85003, China), stopwatch, steel ruler, vernier caliper, storage bags, label, and other tools.

The control and data acquisition system scheme of the bench is shown in Figure 9, which consists of an inverter A (SPD990-G15KW-H3-D, China) controlling the feeding motor, another inverter B (ZK880-30KWG-3, China) controlling chopping motor, a feeding moto (YE2-20CL1-1, China), a chopping motor (YE2-20CL1-2, China), a dynamic torque transducer (JN-DN3, Germany), a measuring and control instrument (MCK-DN, China) and an up computer for human-machine interface (HY-eVision27.0, Germany). Inverter A was used to realize the stepless adjustment of feeding speed and inverter B was used to realize stepless adjustment of the rotating speed of the chopping cylinder. The dynamic torque transducer was mounted between a pair of transition sprockets for the chopping motor and chopping cylinder, which can measure the torque from 0-2000 N m with an accuracy of ±0.5% F.S. (Full Scale) and speed from 0-3000 r/min with an accuracy of ±0.05% F.S. The measuring and control instrument adopts an external 24 DC power supply, and the sampling period is 1000 m s. Data transmission adopts custom protocol or Modbus-RUT protocol with the communication of RS485 half-duplex master-slave mode. The value and curve of rotating speed and torque can be displayed in real-time on the human-machine interface.

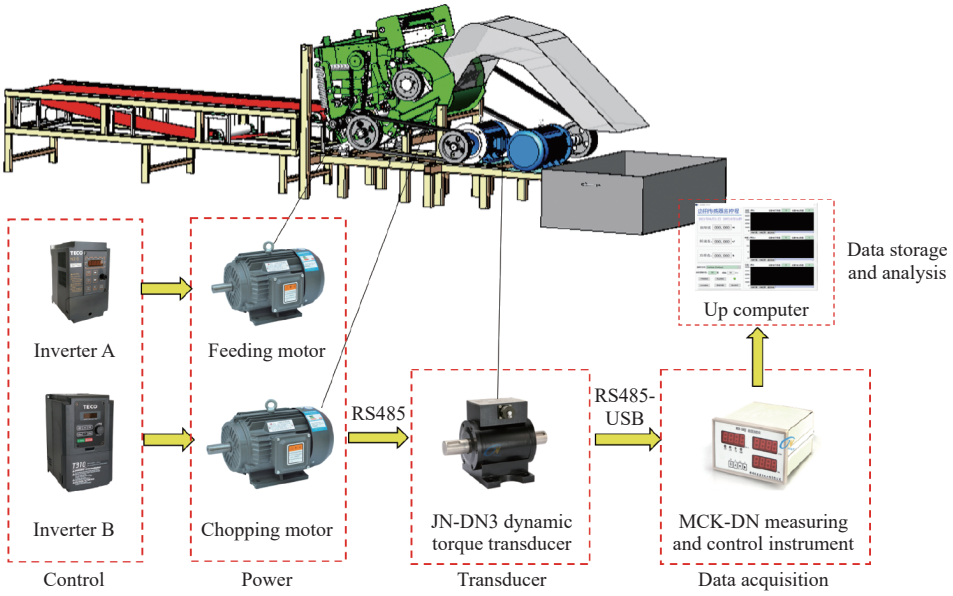

Figure 9 Components of the feeding and chopping data control and acquisition system

4.3 Test methods

In order to reduce operating energy consumption and improve the quality of chopping, feeding speed, rotating speed of the chopping cylinder, and feeding amount were selected as experimental factors. In addition, because the radial shearing in different directions has a significant influence on the shearing power consumption of whole silage maize, the feeding direction was also selected as the experimental factor.

Because the silage maize harvester is not stable in field operation, the theoretical section length of silage maize is usually inconsistent with the actual section length. Therefore, the theoretical and actual section lengths were selected for comparison to analyze whether the influencing factors of the experiments had a significant impact on the actual section length.

According to the performance requirement of feeding and chopping device and the evaluation requirement of harvesting quality of silage maize by self-walking maize harvester. The SGLR Y_1 and ECPUM Y_2 were selected as the evaluation indexes, and the method was carried out according to the *Green Fodder Harvester* (DG/T052-2019). The SGLR was a key index to describe the chopping effect, while the ECPUM was a key index to describe energy consumption of chopping[22].

The theoretical section length is calculated as follows:

$$l_P = 6000 \times \frac{v_W}{nk} \tag{30}$$

where, v_W is the feeding speed of the feeding roller, m/s.

The SGLR is calculated as follows:

$$Y_1 = \frac{G_c}{G_y} \times 100\% \tag{31}$$

where, l_p is the theoretical section length, mm; G_c is the total mass of standard length maize, kg; The standard length maize is grass whose cut grass length is in the range of (0.7-1.2) l_p.

The energy consumption of chopping cylinder is calculated as follows:

$$W_t = T\omega t \times 10^{-3} = 2\pi nt \frac{\sum_{i=1}^{\mu} T_i}{60\mu} \times 10^{-3} \tag{32}$$

where, n is the angle of corresponding to the feeding direction, (°); T_i is the instantaneous torque of chopping cylinder collected at i, N·m; T is the torque of chopping cylinder, N·m; μ is the number of torque data collected in a single test.

$$m_t = w \cdot t \tag{33}$$

where, t is the test time, s; w is the feeding amount, kg.

The ECPUM is calculated as follows:

$$Y_2 = \frac{W_t - W_0}{m_t} \tag{34}$$

where, W_t is the total chopping energy consumption, kJ; W_0 is the idling chopping energy consumption, kJ; m_t is the total mass of test sample, kg;

4.3.1 Single factor test

In order to observe the feeding, conveying, and chopping performance of silage maize and obtain the best working parameters of the optimized feeding and chopping device, it is necessary to conduct a single factor test to determine the best range of working parameters of each device. Based on the theoretical analysis of each experimental factor, preliminary experimental study, and reference to the field operation parameters of silage maize harvesters at home and abroad[6,14], the test level of each factor is listed in Table 2. The combination of single factor test center level was as follows: feeding speed 3.5 m/s, the rotating speed of chopping cylinder 1000 r/min, feeding amount 8 kg/s, and feeding direction 90°. Among them, 90° is the main direction of crop entering the feeding. During the test, the other experiment factors were fixed as the center level, and each group was repeated 3 times, and the average value was taken as the test results.

Table 2 Factors and their levels of single factor test

Levels	Factors			
	Feeding speed/m·s^{-1}	Rotating speed of chopping cylinder/r·min^{-1}	Feeding amount/kg·s^{-1}	Feeding direction/(°)
1	2.0	700	4	0°
2	2.5	800	5	45°
3	3.0	900	6	90°
4	3.5	1000	7	
5	4.0	1100	8	
6	4.5	1200	9	
7			10	

4.3.2 Orthogonal test

In order to further explore the interaction and influence factors on the evaluation indexes, the orthogonal test of feeding and chopping operation parameters of silage maize was carried out[23,24]. On basis of single-factor test results, four-factor three-level response surface tests were carried out, and the factors and levels are listed in Table 3.

Table 3 Factors and levels of orthogonal factor test

Levels	Factors			
	Feeding speed/m·s^{-1}	Rotating speed of chopping cylinder/r·min^{-1}	Feeding amount/kg·s^{-1}	Feeding direction/(°)
−1	3	800	6	0°
0	3.5	1000	8	45°
1	4	1200	10	90°

4.3.3 Field test

The cutting table cannot realize the feeding of plants in specific directions, for the self-propelled silage maize harvester is still a new type. The cutting quality should be tested in field operation, and the SGLR was selected as the evaluation index. The optimal combination of feeding amount, feeding speed, and rotating speed of chopping cylinder in bench test was only tested and verified.

During the test, a total of four trips were determined, two for each trip, and the test data were averaged according to China Local Standard DB13/T23388-2016 (General technical requirements for self-propelled green feed harvesters). SGLR is calculated according to Equation (30). The field test was conducted in a professional planting cooperative in Zibo, Shandong Province in September 2021. The silage maize varieties tested in the field were consistent with those tested on the bench. The row and planting spacing were 600 mm and 200 mm respectively. The test site was 200 m in length and 50 m in width. The average height of silage maize "Zhengdan 958" was 2322 mm, the average diameter of root stalk was 34.2 mm, the height of maize ear was 945 mm, and the moisture content of silage maize was 62.1%, and the plant grew well without lodging. It was the same variety and planting batch as the silage maize in bench test.

5 Results and analysis

5.1 Single factor test

5.1.1 Influence of experimental factors on evaluation index

The influence of experimental factors on SGLR and ECPUM is shown in Figure 10, respectively.

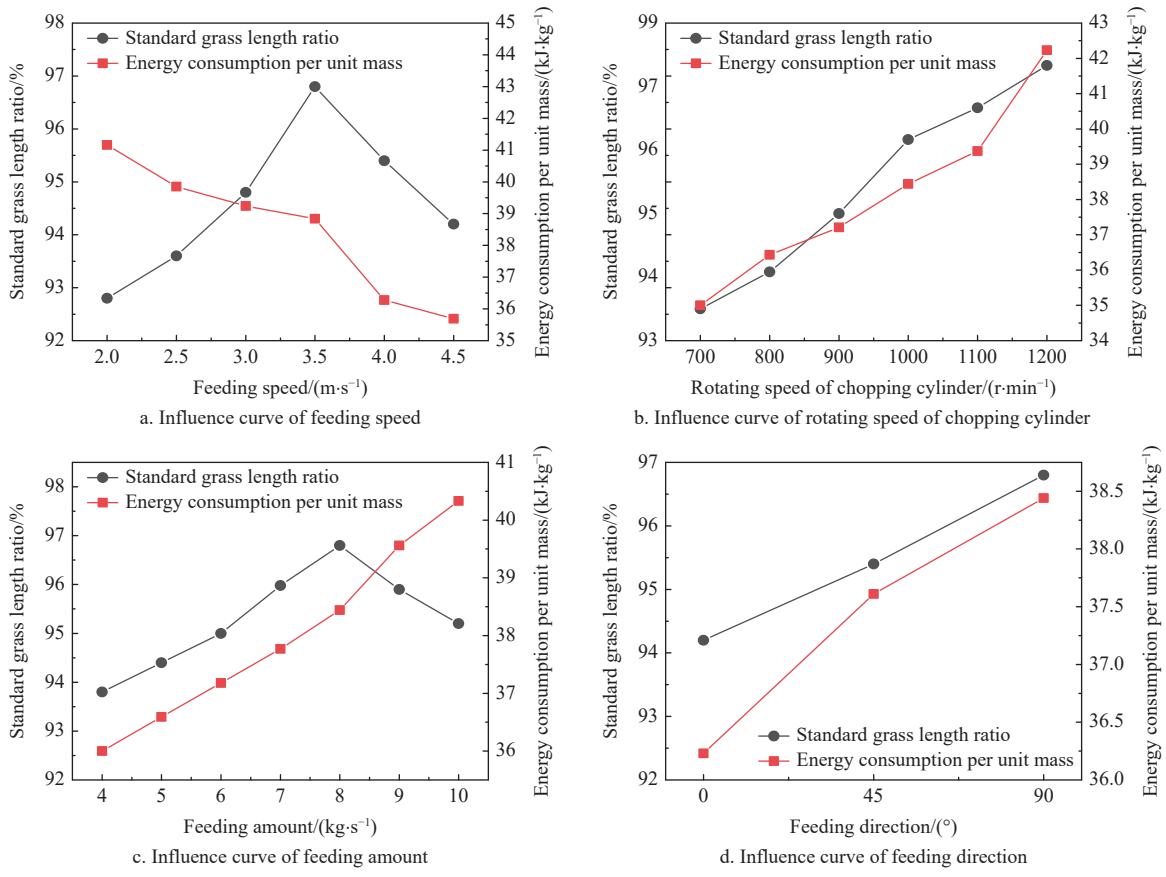

a. Influence curve of feeding speed

b. Influence curve of rotating speed of chopping cylinder

c. Influence curve of feeding amount

d. Influence curve of feeding direction

Figure 10 Changing law of evaluation index with experimental factors

As can be seen from Figure 10a, with the increase of feeding speed, the SGLR increased first and then decreased, while the ECPUM decreased. When the feeding speed was 3.5 m/s, the SGLR reached the peak and then decreased rapidly, while the ECPUM also decreased rapidly. The results showed that the feeding speed had a great influence on the evaluation indexes. If the feeding speed was too high, the SGLR might be reduced because the crops were not cut in time. In order to improve the qualified rate of straw cutting and reduce the energy consumption of chopping, the feeding speed range was determined as 3-4 m/s.

As can be seen from Figure 10b, with the increase in rotating speed, both the two evaluation indexes showed an upward trend, which showed that the rotating speed had a great influence. In particular, when the rotating speed was less than 800 r/min, the SGLR was less than 95%. Therefore, the range of rotating speed of the chopping cylinder was selected as 800-1200 r/min.

As can be seen from Figure 10c, with the increase in feeding amount, the ECPUM increased uniformly, and the SGLR increased first and reached a peak with the feeding amount of 8 kg/s, and then decreased. When the feeding amount exceeded 8 kg/s, the cutting force of the moving blade increased and the chopping effect deteriorates due to the thickness of the feeding layer, resulting in a decrease in the SGLR. When the feeding amount was less than 6 kg/s, the SLGR was less than 95% which cannot meet the design requirements. In order to meet the demand for large feeding amounts, the range of feeding amount was selected as 6-10 kg/s.

As can be seen from Figure 10d, with the change of feeding direction from 0° to 90°, the evaluation indexes both showed an upward trend. In the 0° direction, the energy consumption was the lowest, but the straw quantity satisfying the qualified section length was small. While in the 90° direction, the straw meeting the qualified section length was the largest, but the energy consumption was also high. In order to further study the interaction between feeding direction and other experimental factors on the evaluation indexes, the directions of 0°, 45°, and 90° were selected for further study.

5.1.2 Relationship between theoretical and actual section length and ECPUM

Figure 11 showed the relationship between actual and theoretical section length as well as the relationship between them and ECPUM, based on the single factor tests.

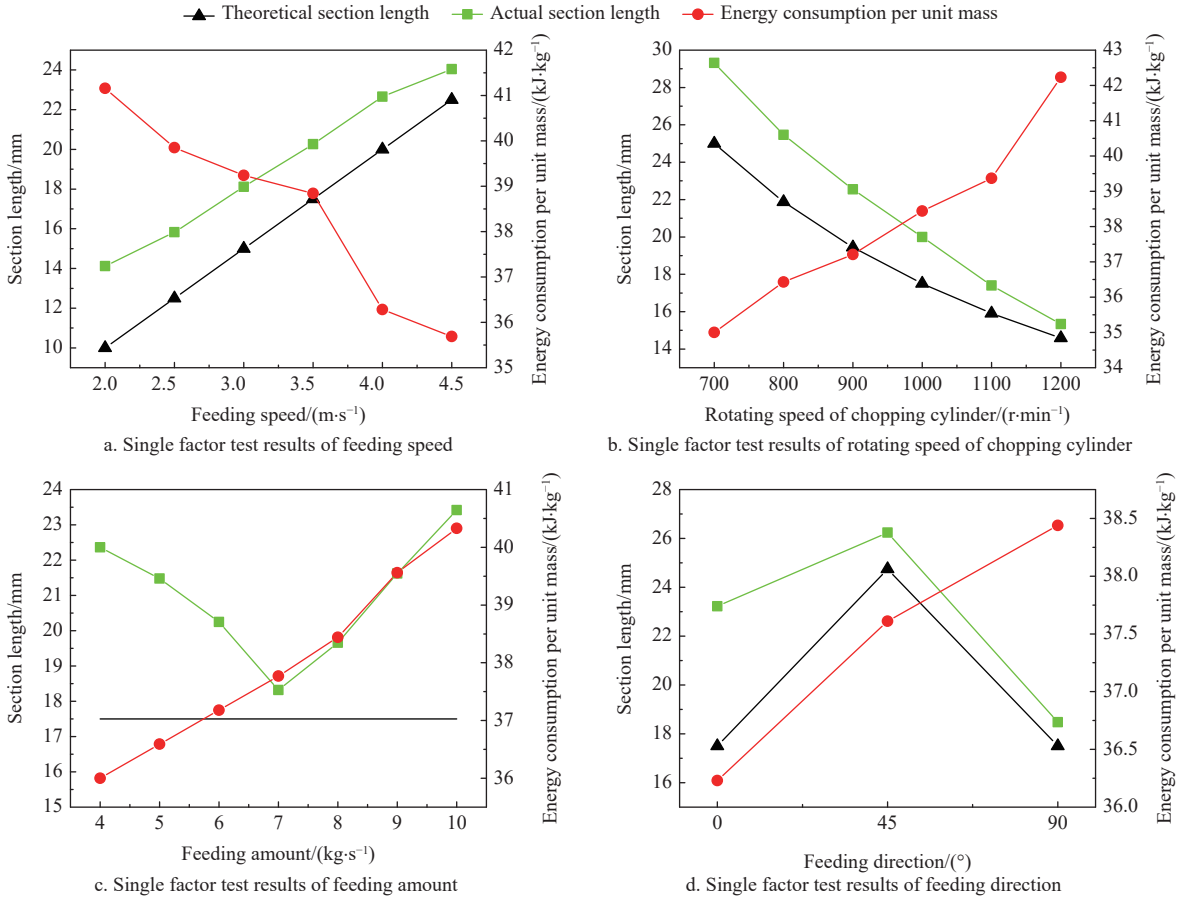

a. Single factor test results of feeding speed

b. Single factor test results of rotating speed of chopping cylinder

c. Single factor test results of feeding amount

d. Single factor test results of feeding direction

Figure 11 Effects of experimental factors on section length and ECPUM

As can be seen from Figure 11a, with the increase in feeding speed, the actual section length was larger than the theoretical length, the ratio between them was smaller and smaller, and the ECPUM decreased with the increase in straw section length. Therefore, proper selection of large feeding speed can ensure the quality of chopping and reduce energy consumption.

As can be seen from Figure 11b, the higher the rotating speed was, the closer the actual section length was to the theoretical section length. As the section length decreased, the frequency of chopping silage maize increased and the energy consumption increased significantly. Therefore, considering that chopping precision and energy consumption cannot be taken into account at the same time, it is necessary to choose the appropriate rotating speed.

As can be seen from Figure 11c, with the increase in feeding amount, the actual section length decreased first and then increased, but was larger than the theoretical section length, while the ECPUM increased gradually. When the feeding amount was 7 kg/s, the actual section length was closest to the theoretical section length, and the coefficient of variation was 3.2%. In particular, when the feeding amount was large, the thickness of the feeding layer increased, and the section length of the lower crop was increased because the section length of the upper silage maize was not as good as the lower silage maize. In conclusion, the feeding amount had a certain influence on the section length of silage maize straw.

As can be seen from Figure 11d, the feeding direction had a significant effect on the section length. The ideal feeding condition was 90° when feeding in 0°direction, the difference between the actual section length and theoretical section length was significantly greater than that in other directions. Although the moving blade rotated along the helical line and formed shearing action with the fixed blade, the straw was easy to tear along the fiber direction in

this direction, resulting in the increase of the actual section length, but the energy consumption was minimum. While in the 45° direction, the variation coefficient of the section length was small, and the consumption was also in the middle level. Therefore, the optimization of the cutting table conveying structure in the future can focus on 45°, and the consumption can be reduced as much as possible on the premise of meeting the requirements of the section length.

Combined with the single factor test results, the actual section length and ECPUM data were fitted as shown in Figure 12 and the fitting function was obtained as:

$$Y_2 = (78.692 \pm 7.682\ 37) \cdot l_P^{(-0.241\ 09 \pm 0.032\ 37)} \tag{35}$$

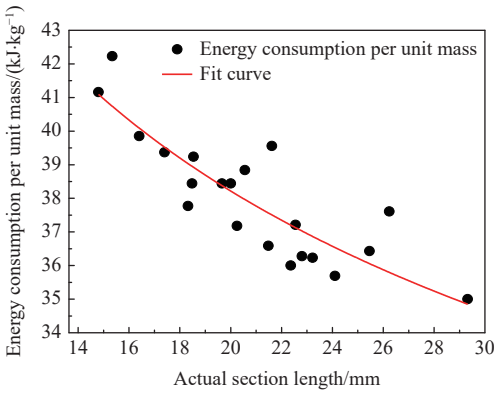

Figure 12 Fitting relationship between actual section length and ECPUM

The fitting coefficient of Equation (35) was 0.742 79, indicating that this function can better fit the relationship between actual section length and ECPUM, and can be used to estimate the impact of section length on the power consumption of the chopping device.

Based on the above analysis, the section length will affect the power consumption of the chopping device. The longer the section length, the lower the power consumption, which was consistent with the empirical Equation deduced[22]. The actual section length was directly proportional to the feeding speed and inversely proportional to the rotating speed of the chopping cylinder, which was similar to and always higher than the theoretical section length. In this structure, the clamping force of the feeding roller can increase the material layer thickness by adjusting the pre-tightening force of the feeding roller spring or increasing the feeding speed.

5.2 Orthogonal test

5.2.1 Establishment of regression model and significance analysis of evaluation index

Design Expert 10.0.3 (Stat-Ease Minneapolis, MN, USA) was used for variance analysis of the test results, and a quadratic polynomial impact surface regression model was established with SGLR (Y_1) and ECPUM (Y_2) as response functions and the feeding speed (X_1), rotating speed of chopping cylinder (X_2), feeding amount (X_3) and feeding direction (X_4) as independent variables, and its significance was tested[15]. The regression equations are shown in Equations (36) and (37), the significance tests of regression equations are listed in Table 4.

$$\begin{aligned} Y_1 = {} & 95.04 + 1.29X_1 + 2.88X_2 + 1.14X_3 + 2.54X_4 - 0.17X_1X_2 - \\ & 1.88X_1X_3 + 0.021X_1X_4 + 0.47X_2X_3 - 0.18X_2X_3 - \\ & 0.88X_3X_4 - 0.74X_1^2 - 0.077X_2^2 - 2.31X_3^2 - 1.15X_4^2 \end{aligned} \tag{36}$$

Table 4 Variance analysis of regression equation for each evaluation index

Items	Sources	Sum of squares	Degree of freedom	Mean square	*F*-values	*p*-values
Y_1	Model	279.81	14	19.99	41.62	<0.0001
	X_1	20.05	1	20.05	41.74	<0.0001
	X_2	99.79	1	99.79	207.80	<0.0001
	X_3	23.91	1	23.91	49.80	<0.0001
	X_4	77.65	1	77.65	161.69	<0.0001
	X_1X_2	0.11	1	0.11	0.23	0.6363
	X_1X_3	14.12	1	14.12	29.40	<0.0001
	X_1X_4	1.806e-003	1	1.806e-003	3.761e-003	0.9520
	X_2X_3	0.90	1	0.90	1.87	0.1931
	X_2X_4	0.13	1	0.13	0.26	0.6164
	X_3X_4	3.06	1	3.06	6.38	0.0242
	X_1^2	3.55	1	3.55	7.40	0.0166
	X_2^2	0.039	1	0.039	0.08	0.7809
	X_3^2	34.70	1	34.70	72.25	<0.0001
	X_4^2	8.54	1	8.54	17.78	0.0009
	Residual	6.72	14	0.48		
	Pure error	1.17	4	0.29		
Y_2	Model	174.19	14	12.44	81.40	<0.0001
	X_1	27.51	1	27.51	180.00	<0.0001
	X_2	69.22	1	69.22	452.83	<0.0001
	X_3	19.74	1	19.74	129.13	<0.0001
	X_4	39.97	1	39.97	261.48	<0.0001
	X_1X_2	0.60	1	0.60	3.93	0.0674
	X_1X_3	2.500E-003	1	2.500E-003	0.016	0.9001
	X_1X_4	0.37	1	0.37	2.43	0.1410
	X_2X_3	0.28	1	0.28	1.84	0.1967
	X_2X_4	0.11	1	0.11	0.69	0.4198
	X_3X_4	1.48	1	1.48	9.66	0.0077
	X_1^2	1.43	1	1.43	9.33	0.0086
	X_2^2	13.78	1	13.78	90.16	<0.0001
	X_3^2	2.86	1	2.86	18.70	0.0007
	X_4^2	0.76	1	0.76	4.98	0.0425
	Residual	2.14	14	0.15		
	Pure error	0.32	4	0.08		

Note: p<0.01(highly significant); 0.01<p<0.05(significant); p≥0.05 (not significant).

$$\begin{aligned} Y_2 = {} & 37.43 + 1.51X_1 + 2.4X_2 + 1.28X_3 + 1.82X_4 + 0.39X_1X_2 + \\ & 0.025X_1X_3 + 0.3X_1X_4 + 0.27X_2X_3 - 0.16X_2X_4 + \\ & 0.61X_3X_4 + 0.47X_1^2 + 1.46X_2^2 + 0.66X_3^2 + 0.34X_4^2 \end{aligned} \tag{37}$$

As can be seen from Table 4, the response surface models for SGLR (Y_1) and ECPUM (Y_2) indicated that the fitting degree of the model was significant (p<0.05). As for the SGLR, the regression terms X_1, X_2, X_3, X_4, X_3^2, X_4^2, and the interaction term X_1, X_3 had a highly significant effect (p<0.01). The impacts of X_1X_2, X_1X_4, X_2X_3, X_2X_4, X_2^2 on the SGLR(Y_1) were not significant (p>0.05). As for the ECPUM, the impacts of terms X_1, X_2, X_3, X_4, X_1^2, X_2^2, X_3^2, X_4^2 and the interaction term X_3X_4 had a highly significant effect (p<0.01), but the interaction terms of X_1X_2, X_1X_3, X_1X_4, X_2X_3 and X_2X_4 were not significant (p>0.05).

With the insignificant factors eliminated, the second-order multiple regression equations for experimental factors are shown in Equations (38) and (39). The P values of the optimized response surface models for SGLR (Y_1) and ECPUM (Y_2) were all less than 0.0001, indicating that the optimized models were very reliable.

$$bY_1 = 94.99 + 1.29X_1 + 2.88X_2 + 1.41X_3 + 2.54X_4 - 1.88X_1 \cdot X_3 - 0.88X_3 \cdot X_4 - 0.73X_1^2 - 2.30X_3^2 - 1.13X_4^2 \quad (38)$$

$$bY_2 = 37.43 + 1.51X_1 + 2.4X_2 + 1.28X_3 + 1.82X_4 + 0.64X_3 \cdot X_4 + 0.47X_1^2 + 1.46X_2^2 + 0.66X_3^2 + 0.34X_4^2 \quad (39)$$

5.2.2 Analysis of interaction results

It can be known from Table 4 that the order of influencing the SGLR (Y_1) was X_2>X_4>X_3>X_1. The response surface diagram was obtained after data processing so as to intuitively analyze the relationship between various experimental factors and chopping performance SGLR as shown in Figure 13.

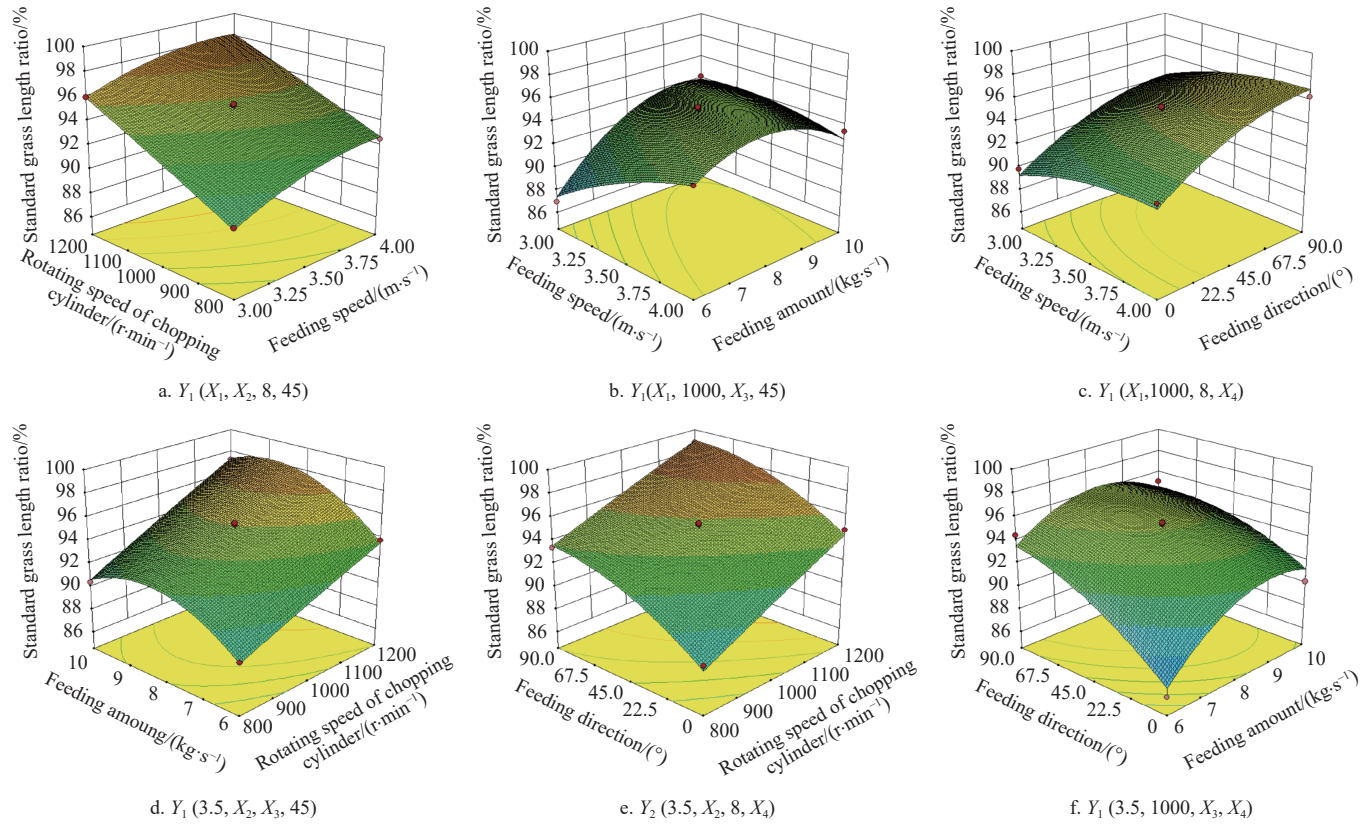

a. Y_1 (X_1, X_2, 8, 45) b. Y_1(X_1, 1000, X_3, 45) c. Y_1 (X_1,1000, 8, X_4)

d. Y_1 (3.5, X_2, X_3, 45) e. Y_2 (3.5, X_2, 8, X_4) f. Y_1 (3.5, 1000, X_3, X_4)

Figure 13 Influence of different factors on SGLR

In Figure 13a, at the same rotating speed of chopping cylinder, the SGLR increased first and then decreased as the feeding speed increased; at the same feeding speed, the SGLR showed a marked upward trend as the rotating speed of chopping cylinder increased. When the rotating speed was small, the effect of chopping was obviously affected by feeding speed. The faster the feeding speed was, the more crops entered per unit time, and it was difficult to chop thick crop layers by moving blade, while the slower the feeding speed was, the smaller the theoretical chopping length was, and longer straws that did not meet the requirements lead to a lower SGLR. In addition, the faster the rotating speed was, the easier it was to chop off the straw, and the chop section was neat.

In Figure 13b, at the same feeding amount, the SGLR increased first and then decreased as the feeding speed increased; at the same feeding speed, the SGLR also increased first and then decreased as the feeding amount increased. The interaction between the two factors was obvious. When the feeding amount and feeding speed were small, the crop layer was thin, and the clamping force of the feeding roller on the crop was small. When the moving blade chopped the crop, it was easy to slip, resulting in the increase of SGLR.

In Figure 13c, at the same feeding direction, the SGLR also increased first and then decreased slowly as the feeding speed increased, at the same feeding speed, the SGLR increased gradually as the feeding direction increased. SGLR was significantly lower in 0° direction than that in other directions, the reason may be that in this direction, longer straw sections were easily pulled out by moving blade at chopping sections. While in 90° directions, the change of section length was minimal. However, the straw entering the chopping device was chaotic due to the structural influence of the harvesting platform and conveying device during actual field harvesting.

In Figure 13d, at the same feeding amount, the SGLR increased quickly as the rotating speed of chopping cylinder increased, and at the same rotating speed, the SGLR also increased first and then decreased as the feeding amount increased, and when the feeding amount was 8 kg/s, the SGLR achieved maximum value. When the rotating speed of chopping cylinder was lower and the feeding amount was larger, the chopping effect was worse.

In Figure 13e, at the same feeding direction, the SGLR increased gradually as the rotating speed of chopping cylinder increased and achieved maximum when the rotating speed was 1200 r/min. At the same rotating speed, the SGLR increased gradually as the feeding direction changed from horizontal to vertical and achieved maximum in 90° direction. Although 0° direction was not conducive to chopping, once the rotating speed is over 1000 r/min, it also can get better sections.

In Figure 13f, at the same feeding direction, the SGLR increased first and then decreased gradually as the feeding amount increased, and the SGLR increased first and then decreased as quickly as the feeding direction changed from horizontal to vertical.

When the feeding amount was small, the effect of feeding direction on the SGLR was more obvious. The lowest value occurred in the 0° direction, which was less than 90%.

To sum up, the rotating speed of chopping cylinder and feeding direction had significant effects on the SGLR. In addition, increasing the feeding amount and feeding speed appropriately can improve the SGLR.

It can be known from Table 4 the order of influencing the ECPUM (Y_2) was $X_2>X_4>X_1>X_3$ The response surface diagram was obtained after data processing so as to intuitively analyze the relationship between various experimental factors and chopping performance ECPUM. As shown in Figure 14.

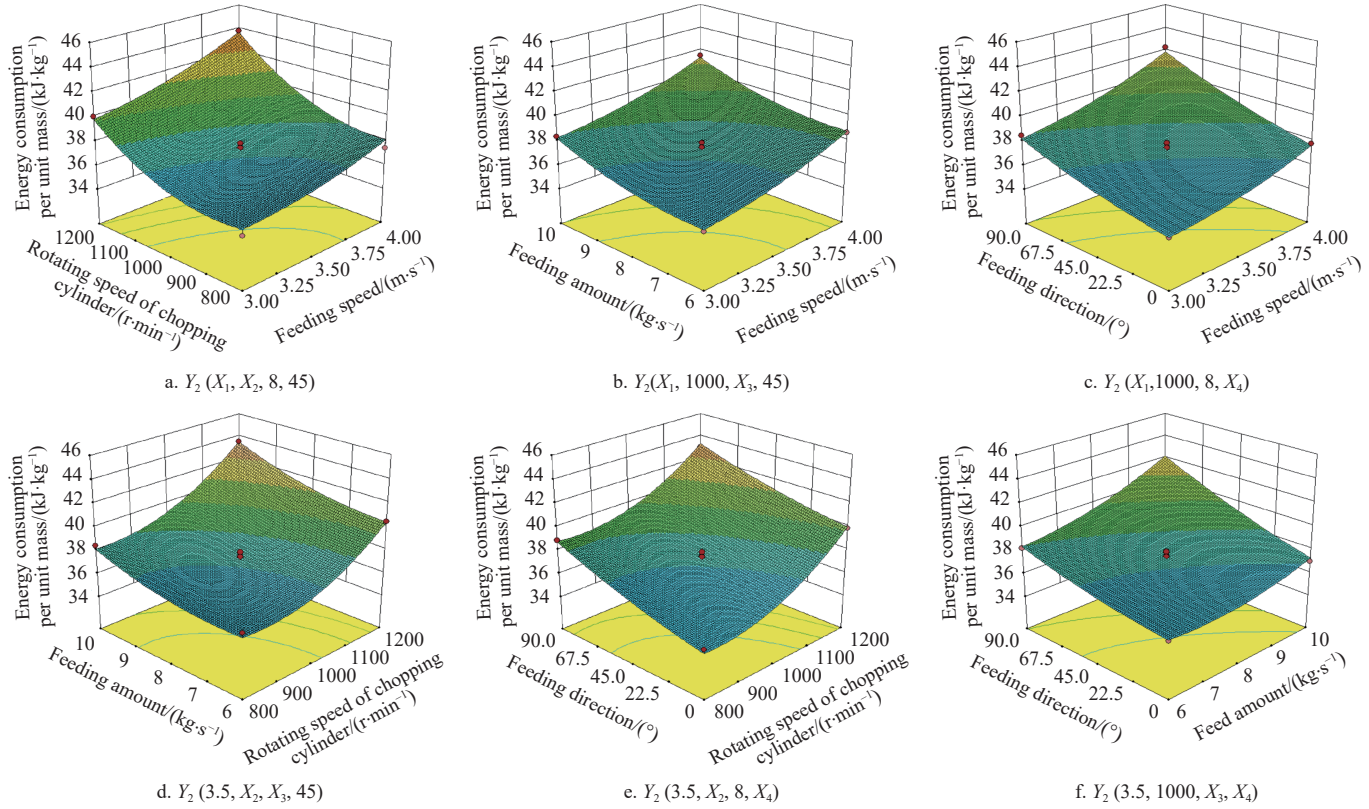

a. Y_2 (X_1, X_2, 8, 45) b. Y_2(X_1, 1000, X_3, 45) c. Y_2 (X_1,1000, 8, X_4)

d. Y_2 (3.5, X_2, X_3, 45) e. Y_2 (3.5, X_2, 8, X_4) f. Y_2 (3.5, 1000, X_3, X_4)

Figure 14 Influence of different factors on ECPUM

In Figure 14a, at the same feeding speed, the ECPUM showed a clear upward trend as the rotating speed of chopping cylinder, and at the same rotating speed of chopping cylinder, the ECPUM showed a relatively slow upward trend as the feeding speed increased. According to the empirical Equation of the power consumption of the chopping device, the rotating speed had a square or cubic influence on the consumption of accelerating crop transportation, overcoming the friction between the crop and the chopping drum, and transporting the chopped crop backward. Therefore, the greater the rotating speed, the greater the power consumption. Therefore, the power consumption was very high even when the feeding amount was low. The faster the feeding speed was, the more crops need to be cut per unit time, and the greater the chopping force required. Therefore, the ECPUM increased with the feeding speed.

In Figure 14b, at the same feeding amount, the ECPUM increased gradually as the feeding speed increased, and at the same feeding speed, the ECPUM showed an upward trend as the feeding amount increased. The thickness of chopped crop layer per unit time was similar at low feeding amount with high feeding speed or high feeding amount with low feeding speed, so there was a certain interaction between these two factors. At the same time, the influence of the two factors on the SGLR can provide a theoretical basis for reducing the power consumption of chopping and improving the chopping quality.

In Figure 14c, at the same feeding direction, the ECPUM increased gradually as the feeding speed increased, and at the same feeding direction, the ECPUM showed a clear upward trend. The feeding direction had an obvious influence on ECPUM, mainly affected by the structure and mechanical and physical characteristics of the straw. When feeding at 3 m/s in 0° direction, the minimum ECPUM was achieved.

In Figure 14d, at the same feeding amount, the ECPUM increased rapidly as the rotating speed of chopping cylinder increased, and at the same rotating speed, the ECPUM increased gradually as the feeding amount increased. Even when the feeding amount was low, the higher rotating speed would lead to a higher ECPUM. Therefore, on the premise of guaranteeing the SGLR, the operation power consumption of the chopping device can be reduced by appropriately reducing the rotating speed of the chopping cylinder.

In Figure 14e, at the same direction, the ECPUM increased rapidly as the rotating speed of chopping cylinder increased, and at the same rotating speed, the ECPUM increased gradually as the feeding direction increased. The effect of feeding direction was more obvious when the rotating speed of the chopping cylinder was lower.

In Figure 14f, at the same feeding direction, the ECPUM increased gradually as the feeding amount increased, and at the same feeding amount, the ECPUM increased gradually as the change of feeding direction from transverse to longitudinal. The ECPUM was most significantly affected by feeding direction at the

feeding amount of 10 kg/s. The ECPUM achieved the minimum value at the feeding amount of 6 kg/s in 0° direction.

To sum up, the increase in feeding speed, rotating speed of chopping cylinder, and feeding amount had positive correlation with the ECPUM, and negative with ECPUM when the feeding direction changed from transverse to longitudinal. Therefore, it was helpful to reduce the working energy consumption of chopping device when properly reducing the feeding speed, rotating speed, and feeding amount, and feeding in a 0° direction.

5.2.3 Parameter optimization and test verification

Through a Box-Behnken simulation test, the optimal combination of the parameters influencing the feeding and chopping of silage maize was determined, thereby achieving the best performance of self-working silage maize harvester feeding and chopping device, improving the qualified rate of chopping section and reducing operation power consumption. Because of the influence of the various factors on the target value, a global multi-objective optimization was necessary[21]. The optimal constraint was as follows:

$$\begin{cases} \max Y_1 \\ \min Y_2 \\ \text{s.t} \begin{cases} 3.5\ \text{m/s} \le X_1 \le 4\ \text{m/s} \\ 800\ \text{r/min} \le X_2 \le 1200\ \text{r/min} \\ 6\ \text{kg/s} \le X_3 \le 10\ \text{kg/s} \\ 0^\circ \le X_4 \le 90^\circ \end{cases} \end{cases} \tag{40}$$

Through the solution of the Design-Expert software, the best combination was found. When the feeding speed, rotating speed of the chopping cylinder, feeding amount, and feeding direction were 3.39 m/s, 1016.17 r/min, 8.04 kg/s, and 52.2°, SGLR and ECPUM were 95.35%, and 37.63 kJ/kg.

To verify the accuracy of the optimized model, the parameters of the optimized factors were tested on the bench site. Considering the practical application of the bench, the above parameters were taken as follows: the feeding speed was 3.4 m/s, the rotating speed of chopping cylinder was 1015 r/min, the feeding amount was 8 kg/s, and the feeding direction was 50°. The experiment was repeated 10 times with the optimized parameters, and the results are listed in Table 5.

Table 5 Comparison between model optimization and validation test value

Item	Evaluation index	
	Y_1/%	Y_2/kJ·kg^{-1}
Model optimization value	95.35	37.63
Validation test value	94.55	38.75
Relative error/%	0.94	2.97

In the comparison of the predicted result and experimental result, the relative errors of all property indexes were less than 5%, which showed that the established model was reliable and could be used for prediction and optimization. From the data in Table 5, it can be found when the feeding amount was 8 kg/s, the SGLR was 94.55%, and the ECPUM was 38.75 kJ/kg, which can meet the operation demands of large feeding amount of domestic self-propelled silage maize harvester. Huang et al.[24] developed a combined device of four-rollers feeding and plate moving blade cutter, and when the rotating speed of the chopping cylinder was 1000 r/min. the SGLR was only 90.3%. Shen et al developed a chopping device for silage maize harvester, and when the rotating speed of the chopping cylinder was 1200 r/min, the SGLR was 93.1%, and the energy consumption ratio was 7.85 kW·h/t[21].

In conclusion, by optimizing the structure and working parameters of the feeding and chopping device of the traditional silage maize harvester, the chopping energy consumption can be significantly reduced and the chopping quality can be improved, which provides a reference for the optimization and improvement of the key device of the silage maize harvester.

5.3 Field test

Field test was made with working speed of 5.4 m/s, and the corresponding feeding amount reached 8 kg/s. The test would start after the silage maize harvester run smoothly, as shown in Figure 15.

Figure 15 Field test

The measurement process was shown in Figure 16. The maturity of the silage maize was not consistent, there were many furrows in the field, the walking speed was not stable and other factors led to the fluctuation of the silage maize harvester feeding amount, the average SGLR was 93.28%.

1. Sampling 2. Qualified samples 3. Unqualified straw 4. Unbroken grains

Figure 16 Test results measurement process

In field operation, the different diameter five-rollers feeding device and plate hob chopping device run smoothly. The flow of silage maize was smooth and there was no clogging phenomenon. The field test showed that the feeding device and chopping device could realize the functions of grabbing, evenly conveying, feeding and chopping off the feeding, which improved the field adaptability of the silage maize harvester and could meet the working requirements of the silage maize harvester with a large feeding amount.

6 Conclusions

A horizontal different diameters five-rollers feeding device (HDDFD) was designed to solve the problem of feeding blockage with the diameter of the up roller larger than the low roller. The moving and fixed blade was rearranged to make the actual cutting-edge curve the closer to the theoretical cutting-edge curve which can help to reduce the cutting energy consumption and improve the cutting quality.

The single factor test determined the optimal range of feeding speed, rotating speed of chopping cylinder, feeding amount, and

feeding direction, compared and analyzed the relationship between actual section length and ECPUM. Using the Box-Behnken design, the response surface regression model of the SGLR and ECPUM was established. Through variance and response surface analysis, the effects of factors were studied. When the feeding speed was 3.39 m/s, the rotating speed of chopping cylinder was 1016.17 r/min, the feeding amount was 8.04 kg/s, and the feeding direction was 52.2°, the SGLR and ECPUM were 95.35%, 37.63 kJ/kg. Field tests have verified the reliability of the optimized feeding and chopping device. All the indexes were better than the relevant national standards and existing silage maize harvesters made in China. Therefore, the research results of this paper can be used to optimize the feeding and chopping device of silage maize harvester.

Acknowledgements

The research program is supported by the Key Science and Technology Innovation Project of Shandong Province, China (Grant No. 2019JZZY020615), and the Shandong Province Agricultural major application technology innovation project (Grant No. SD2019NJ005).

[References]

[1] Jamshidpouya M, Najafi G, Tavakoli Hashjin T. Design, fabrication and evaluation of electric forage chopper with adjustable helix angle. Journal of Agricultural Science and Technology, 2018; 20(5): 923–938.

[2] Geng D Y, Mu X D, Sun Y C, Zhang Y M, Li H B, Jiang H X. Simulation and test of silage corn screw notched sawtooth type crushing roller. Transactions of the CSAM, 2021; 52(12): 134–141. (in Chinese)

[3] Cong H B, Yao Z L, Zhao L X, Meng H B, Wang J C, Huo L L, et al. Distribution of crop straw resources and its industrial system and utilization path in China. Transactions of the CSAE, 2019; 35(22): 132–140. (in Chinese)

[4] Zhang Z L, Han Z D, Li X D, Hao F P, Han K L, Han L J. Optimization of parameters for stalk chopper of corn harvester for reaping both corn stalk and spike. Journal of Agricultural Machinery, 2018; 49(S1): 273–281. (in Chinese)

[5] Zhu X L, Chi R J, Du Y F, Qin J H, Xiong Z X, Zhang W T, et al. Experimental study on the key factors of low-loss threshing of high-moisture maize. Int J Agric & Biol Eng, 2020; 13(5): 23–31.

[6] Mou X, Jiang H, Sun Y. Simulation optimization and experiment of disc-type grain crushing device of silage corn harvester. Transactions of the CSAM, 2020; 5(1): 218–226. (in Chinese)

[7] Zhang F W, Song X F, Zhang X K, Zhang F Y, Wei W C, Dai F. Simulation and experiment on mechanical characteristics of kneading and crushing process of corn straw. Transactions of the CSAE, 2019; 35(9): 58–65. (in Chinese)

[8] Wang G, Jia H L, Tang L, Zhuang J, Jiang X M, Guo M Z. Design of variable screw pitch rib snapping roller and residue cutter for corn harvesters. Int J Agric & Biol Eng, 2016; 9(1): 27–34.

[9] Wan X Y, Liao Q X, Jiang Y J, Liao Y T. Cattle feeding experiment and chopping device parameter determination for mechanized harvesting of forage rape crop. Transactions of the ASABE, 2021; 64(2): 715–725.

[10] Hou L Y, Wang K R, Wang Y Z, Li L L, Ming B, Xie R Z. In-field harvest loss of mechanically-harvested maize grain and affecting factors in China. Int J Agric & Biol Eng, 2021; 14(1): 29–37.

[11] Ma P B, Li L Q, Wen B Q, Xue Y H, Kan Z, Li J B. Design and parameter optimization of spiral-dragon type straw chopping test rig. Int J Agric & Biol Eng, 2020; 13(1): 47–56.

[12] Wan Q, Wang D, Wang G, Gong Z Q, Bai Y. Design and experiment of self-propelled grass silage combined bagging machine. Transactions of the CSAE, 2014; 30(19): 30–37. (in Chinese)

[13] Zhang Z, Chi R J, Du Y F, Pan X, Dong N X, Xie B. Experiments and modeling of mechanism analysis of maize picking loss. Int J Agric & Biol Eng, 2021; 14(1): 11–19.

[14] Wang W W, Li J C, Chen L Q, Qi H J, Liang X T. Effects of key parameters of straw chopping device on qualified rate, non-uniformity and power consumption. Int J Agric & Biol Eng, 2018; 11(1): 122–128.

[15] Zhou H, Zhang J M, Xia J F, Tahir H M, Zhu Y H, Zhang C L. Effects of subsoiling on working quality and total power consumption for high stubble straw returning machine. Int J Agric & Biol Eng, 2019; 12(4): 56–62.

[16] Igathinathane C, Womac A R, Sokhansanj S. Corn stalk orientation effect on mechanical cutting. Biosystems Engineering, 2010; 107(2): 97–106.

[17] Bochat A, Zastempowski M. Comparative study of rape straw cutting with two drum cutting assemblies. Transactions of the ASABE, 2020; 63(2): 345–350.

[18] Wu Z, Gao H, Zhang J. Study on cutting velocity and power requirement in a maize stalk chopping process. Transactions of the CSAM, 2001; 32(2): 38–41. (in Chinese)

[19] Zhang L X, Yang Z P, Zhang Q, Guo H L. Tensile properties of maize stalk rind. BioResources, 2016; 11(3): 6151–6161.

[20] Qi J T, Meng H W, Kan Z, Li C S, Li Y P. Analysis and test of feeding performance of dual-spiral cow feeding device based on EDEM. Transactions of the CSAE, 2017; 33(24): 65–71. (in Chinese)

[21] Shen C, Zhang B, Li X W, Yin G D, Chen Q M, Xia C H. Bench cutting tests and analysis for harvesting hemp stalk. Int J Agric & Biol Eng, 2017; 10(6): 56–67.

[22] Lu Y, Payen S, Ledgard S, et al. Components of feed affecting water footprint of feedlot dairy farm systems in Northern China. Journal of Cleaner Production, 2018; 183: 208–219.

[23] Cui Y J, Wang W Q, Wang M H, Ma Y D, Fu L S. Effects of cutter parameters on shearing stress for lettuce harvesting using a specially developed fixture. Int J Agric & Biol Eng, 2021; 14(4): 152–158.

[24] Huang J C, Tian K P, Shen C, Zhang B, Liu H L, Chen Q M, et al. Design and parameters optimization for cutting-conveying mechanism of ramie combine harvester. Int J Agric & Biol Eng, 2020; 13(6): 94–103.